ELSEVIER

Ceramics International 30 (2004) 927–930

CERAMICS INTERNATIONAL

www.elsevier.com/locate/ceramint

Crystallization kinetics of $MgO–Al_2O_3–SiO_2$ glass-ceramics

Hua Shao*, Kaiming Liang, Fei Peng

Department of Materials Science and Engineering, Tsinghua University, Beijing 100084, PR China

Received 27 June 2003; received in revised form 25 August 2003; accepted 17 October 2003

Available online 10 March 2004

Abstract

The crystallization behavior and microstructure of $MgO–Al_2O_3–SiO_2$ glasses containing TiO_2 were investigated by means of differential thermal analysis (DTA), X-ray diffraction (XRD) and scanning electron microscopy (SEM). The crystallization kinetic parameters including the crystallization apparent activation energy (E) and the Avrami parameter (n) were also measured with Ozawa and Kissinger methods. The results have shown that: The glass first underwent extensive phase separation into titanium-rich droplets in a silica-rich matrix, then magnesium aluminotitanate (MAT) initially precipitated in the droplet phase. As a result the E values of cordierite was decreased, thus the formation of cordierite crystals were promoted.

Keywords: D. Cordierite; D. Glass-ceramics; DTA; Crystallization kinetics

1. Introduction

Currently there has been a considerable amount of interest in cordierite-based glass-ceramics due to their beneficial properties, e.g., good mechanical properties (strength of ∼250 MPa and modulus of ∼150 GPa), low dielectric constant (5.0 at 1 MHz) and low thermal expansion coefficient (about $30\times10^{-7}/^{\circ}C$) [1–4]. The properties of glass-ceramics are dependant on the chemical composition and the thermal history. It is therefore important to gain a thorough understanding of the processes in the crystallization of the glass-ceramics. Although a number of studies have been reported aimed specifically at examining the crystallization mechanisms of cordierite-based glasses [5–9] and in determining the kinetic parameters [10–12], more comprehensive data is required before a clearer understanding of the crystallization process can emerge.

In the present investigation, the nucleation and crystallization sequences of cordierite-based glass-ceramics powder containing a certain amount of TiO_2 were studied and the crystallization kinetics were examined by means of X-ray powder diffraction (XRD) and differential thermal analysis (DTA).

2. Experimental procedure

2.1. Samples preparation

The chemical composition of the glass in the paper in weight is MgO 11–14%, Al_2O_3 30–35%, SiO_2 45–50%, which corresponds to the stoichiometric cordierite, by adding 0.5% Sb_2O_3 and 1% NH_4NO_3 as fluxes, 5% TiO_2 as a nucleating agent. Powder mixtures of reagent grade chemicals were melted in a platinum crucible in an electric furnace at 1600 °C for 2 h. The melts were poured onto 300 °C hot stainless steel plate, transferred to an annealing furnace and held at 500 °C for 1 h, then crushed and remelted at least three times to ensure homogeneity.

2.2. Differential thermal analysis (DTA)

The resulting glass was crushed and sieved through a 200 mesh to produce glass powder suitable for DTA employing a Dupont DTA with the temperature range of 20–1400 °C. The glass powder with the weight of 50 mg was contained in a platinum crucible and the reference material was α-Al_2O_3 powders. The data were recorded by means of a chart recorder. The samples were heated in air from ambient temperature to 1300 °C at heating rates of 5, 10, 15, 20 K min^{-1}.

* Corresponding author. Tel.: +86-10-62773392.
E-mail address: sh00@mails.tsinghua.edu.cn (H. Shao).

0272-8842/$30.00
doi:10.1016/j.ceramint.2003.10.015

2.3. X-ray powder diffraction (XRD)

The amount and types of crystalline phases existing in a sample after heat treatment were determined by XRD (D/max-RB) using Cu Kα radiation, working voltage 40 kV, working current 80 mA, scanning speed of 4 min^{-1}.

2.4. Scanning electron microscopy (SEM)

After crystallization, the samples were polished and etched in 1% hydrofluoric acid for 30 s (20 °C), then washed, dried and coated with gold in an ion beam coater, and analyzed by SEM (Hitachi S-450).

3. Results and discussion

The relationship between fraction crystallization and the nucleation and growth rates is described by the Johnson–Mehl–Avrami transformation kinetics [13].

$$-\ln\alpha(1-x) = kt^n \quad (1)$$

where x is the fraction crystallized at a given temperature in time t; n is the Avrami exponent which is dimensionless constant related to the nucleation and growth mechanisms; k is the reaction rate constant, which is related to the activation energy, E.

A widely used non-isothermal method is the Ozawa plot [14]

$$\ln\alpha = -\frac{E}{R}\frac{1}{T_P} + C_1 \quad (2)$$

where C_1 is a constant, α is the heating rate in the DTA, E is the crystallization activation energy, T_P is the absolute temperature in DTA curves. A plot of $\ln\alpha$ versus $1/T_P$ is expected to be linear. So activation energy, E, can be attained via this expression.

Another widely used non-isothermal method is the Kissinger plot described as the following equation [15]

$$\ln\frac{T_P^2}{\alpha} = \frac{E}{RT_P} + \ln\frac{E}{R} - \ln v \quad (3)$$

Plot of $\ln(T_P^2/\alpha)$ versus $1/T_P$ also is expected to be linear, and from the slop of the plot, the activation energy, E, can be calculated.

The value of n can be attained from the following equation [16,17]

$$\ln(\Delta T) = -\frac{nE}{R}\frac{1}{T_i} + C_2 \quad (4)$$

Here T_i is the random temperature in the DTA curves, ΔT is the vertical displacement from the baseline to the line of the crystallization exothermic peak at the temperature T_i.

Typical DTA traces of the samples crystallized at heating rates of 5, 10, 15, 20 K min^{-1} are shown in Fig. 1. The glass transition temperature (T_g) of all the curves was evidently about 800 °C. The DTA curves exhibited two distinct exothermic peaks indicating the formation of two crystalline phases, respectively. Table 1 shows the values of the crystallization peak temperature (T_P) of DTA experiments of samples at different heating rates. When the heating rate was 20 K min^{-1}, two exothermic peaks exhibited at 1030 and 1120 °C, respectively.

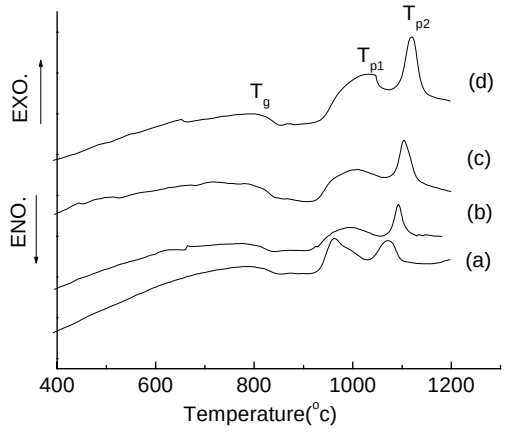

Fig. 1. DTA curves of the glass samples at heating rates of (a) 5 K min^{-1}, (b) 10 K min^{-1}, (c) 15 K min^{-1}, (d) 20 K min^{-1}.

Table 1
The values of T_P (K) at different heating rates α of DTA

Heating rates (K min^{-1})	T_P^1	T_P^2
5	1235	1343
10	1267	1366
15	1280	1376
20	1303	1393

The crystallization of the glass subjected to heat-treatment at 800 °C for 2 h presented typical X-ray pattern characteristic of glass structure as shown in Fig. 2(a). X-ray diffraction showed that the exotherm at 1030 °C corresponds to the crystallization of magnesium aluminotitanate (MAT) as shown in Fig. 2(b), whereas that at 1120 °C was caused by

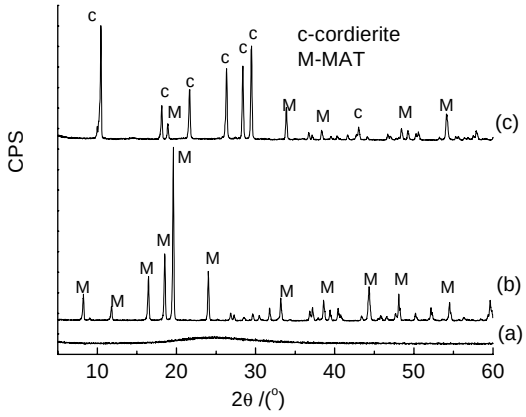

Fig. 2. XRD patterns of sample heated at different heat treatment conditions (a) 800 °C for 2 h, (b)1030 °C for 2 h, (c)1120 °C for 2 h.

Table 2
The values of activation energy E and Avrami parameter n

Crystalline phase	E (kJ mol^{-1})		n			
	Ozawa method	Kissinger method	$\alpha = 5\,\mathrm{K\,min^{-1}}$	$\alpha = 10\,\mathrm{K\,min^{-1}}$	$\alpha = 15\,\mathrm{K\,min^{-1}}$	$\alpha = 20\,\mathrm{K\,min^{-1}}$
MAT	271	251	–	–	–	–
Cordierite	473	433	1.41	1.35	1.46	1.31

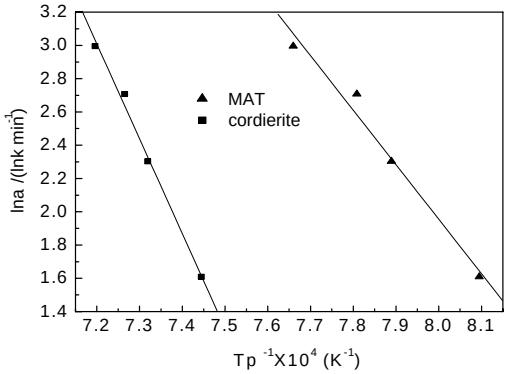

Fig. 3. Plots of $\ln\alpha$ vs. $1/T_P$ for the glass samples.

transformation of metastable MAT into cordierite phase as shown in Fig. 2(c).

Table 2 lists the E values of MAT and cordierite calculated from the slope of $\ln\alpha$ versus $1/T_P$ curves shown in

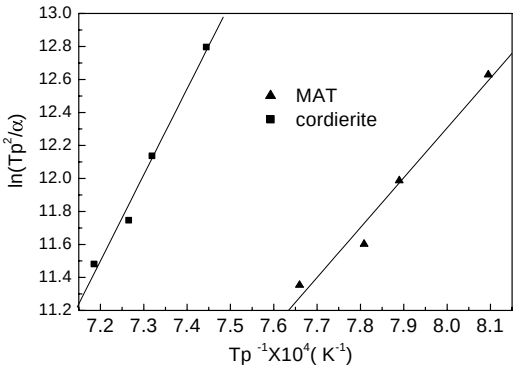

Fig. 4. Plots of $\ln(T_P^2/\alpha)$ vs. $1/T_P$ for the glass samples.

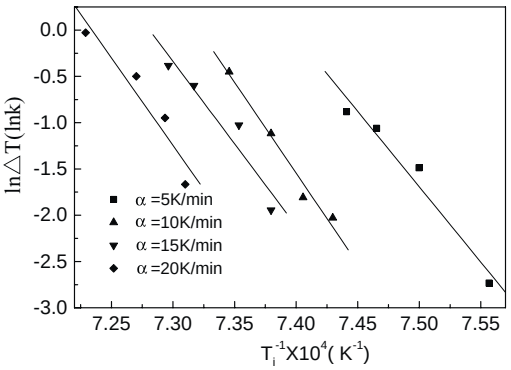

Fig. 5. Plots of $\ln\Delta T$ vs. $1/T_i$ for the glass samples at heating rates of 5, 10, 15, 20 K min^{-1}.

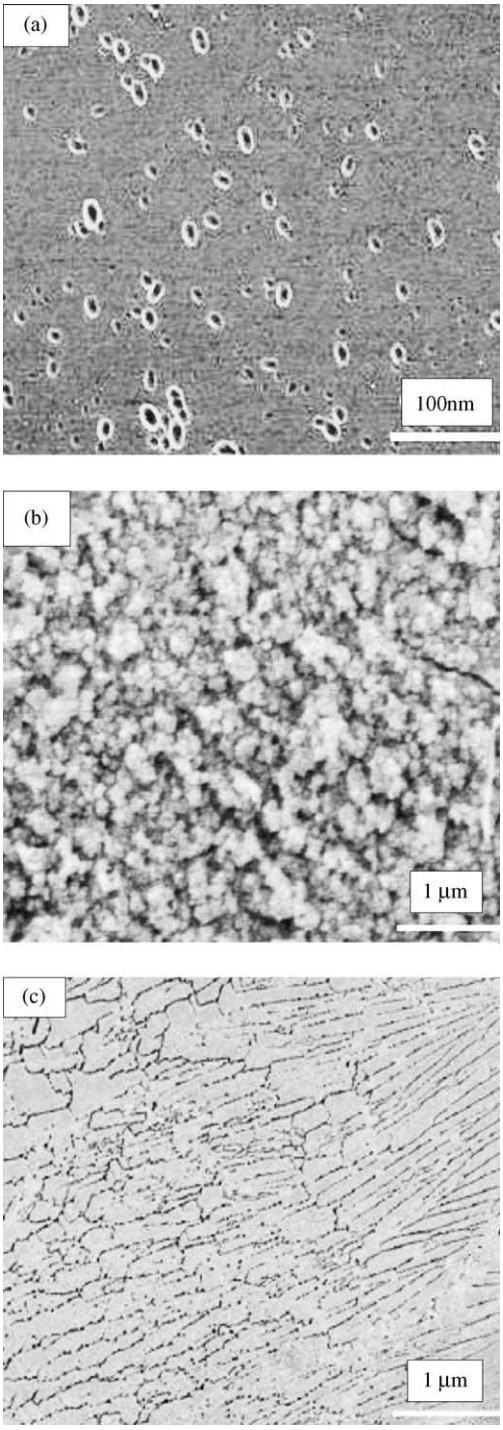

Fig. 6. SEM micrographs of samples at different heat treatment conditions (a) 800 °C for 2 h, (b) 1030 °C for 2 h, (c) 1120 °C for 2 h.

Fig. 3 and from the slope of ln (T_p^2/α) versus $1/T_p$ curves shown in Fig. 4. The apparent activation energies for crystallization of the individual MAT and cordierite phases, determined using Ozawa and Kissinger methods, were in the range of 251–71 and 433–473 kJ mol^{-1}, respectively, which indicated that the formation of the initial crystalline MAT phase from the glass was favored for kinetic reasons [15,16]. Yun-mo sung [18] studied the effect of different additives on the crystallization of cordierite glass-ceramics and determined the apparent activation energy of stoichiometric $2MgO–2Al_2O_3–5SiO_2$ glass as 868 ± 5 kJ mol^{-1}, which was higher than the results obtained in the present paper, indicating the precipitated MAT decreased the apparent activation energy of cordierite and promoted the crystallization of cordierite. Table 2 shows parameter, n, which is determined from the slope of ln ΔT versus $1/T_p$ curves shown in Fig. 5 assure values $n \sim 1$, which means the interface reaction at the droplet in present investigation [13,14].

The samples heat treated at 800 °C for 2 h first underwent extensive phase separation into titanium-rich droplets in a silica-rich matrix shown in Fig. 6(a). No crystalline phase made its appearance confirmed by the results of XRD as shown in Fig. 2(a). There are two possible routes for phase separation [19]: by a nucleation and growth process or by spinodal decomposition. It was observed from the Fig. 6(a) that the droplets form of the second phase and the low interconnectivity of both phases clearly suggested that a nucleation and growth process could be responsible for its development.

Fig. 6(b) shows SEM micrograph of sample heated at 1030 °C for 2 h. The initial MAT made its appearance from the titanite-rich zone which was confirmed by the result of XRD as shown in Fig. 2(b). The morphology of the samples shown in Fig. 6(b) were two-dimensional plate-like precipitation throughout the glass matrix. Zarzychi [20] has put forward the idea that in potassium and caesium titanate glasses Ti does in fact assume a sixfold coordination—state not allowed by the Zachariasen–Warren model of glass structure. Pavlushkin and Khodakovskya [21] have suggested that at high temperatures the Ti^{4+} will assume four-fold co-ordination with oxygen and in this case the titanium–oxygen groups will be structurally compatible with silicate networks. During cooling, the titanium ion will tend to revert to its low temperature equilibrium co-ordination number (six) and will thus be displaced from the silicate network. In combination with a divalent metal oxide, titanium dioxide is therefore likely to form a separate phase. And Schreyer and Schairer [22] are of opinion that the complex magnesium aluminotitanates are formed in the initial stages of devitrification. Fig. 6(c) shows SEM micrograph of sample heated at 1120 °C for 2 h. The average crystal size is 1 μm and the maximal crystal size is about 3 μm.

4. Conclusion

The crystallization apparent activation energies of the individual MAT and cordierite phases, determined using Ozawa and Kissinger methods, were in the range of 251–271 and 433–473 kJ mol^{-1} respectively. The glass first underwent extensive phase separation into titanium-rich droplets in a silica-rich matrix, then magnesium aluminotitanate (MAT) initially precipitated from the droplet phase. And consequently the crystallization apparent activation energy of cordierite was decreased, thus the formation of cordierite crystals were enhanced.

References

[1] A.G. Gregory, T.J. Veasey, J. Mater. Sci. 6 (1971) 1312.
[2] S.H. Knickerbocker, A.H. Kumar, L.W. Herron, Am. Ceram. Soc. Bull. 72 (1993) 90.
[3] M. Sales, J. Alarcon, J. Mater. Sci. 30 (1995) 2341.
[4] R.R. Tummala, J. Am. Ceram. Soc. 74 (1991) 895.
[5] M.A. Mccoy, A.H. Heuer, J. Am. Ceram. Soc. 71 (1988) 673.
[6] M. Awano, H. Takas, Y. Kumahara, J. Am. Ceram. Soc. 35 (1992) 2535.
[7] A.G. Gregory, T.J. Veasey, J. Mater. Sci. 8 (1973) 324.
[8] Y. Hirose, H. Doi, O. Kamigaito, J. Mater. Sci. Lett. 3 (1984) 153.
[9] R. Morrell, Proc. Br. Ceram. Soc. 28 (1979) 53.
[10] R. Muller, J. Therm. Anal. 35 (1989) 823.
[11] P. Amista, M. Cesari, A. Montenero, et al., J. Non-Cryst. Solids. 192/193 (1995) 529.
[12] S.-B. Sohn, S.-Y. Choi, J. Non-Cryst. Solids. 282 (2001) 221.
[13] W.A. Johnson, R.F. Mehl, Trans. AIME. 135 (1939) 416.
[14] T. Ozawa, Polymer 12 (1971) 150.
[15] H.E. Kissinger, J. Res. Natl. Bur. Stand. 57 (1956) 217.
[16] M. Avrami, J. Chem. Phys. 7 (1939) 1103.
[17] G.O. Piloyan, I.D. Ryabchikov, O.S. Novikova, Nature (London) 212 (1966) 1229.
[18] S. Yun -mo, J. Mater. Sci. 31 (1996) 5421.
[19] P.W. Mcmillan, Glass-Ceramics, 2nd edition, Academic Press, London, 1979, p. 74.
[20] J. Zarzychi, J. Mater. Sci. 192 (1971).
[21] N.M. Pavlushkin, R.Ya. Khodakovskaya, Inorg. Mater. Consultants Bur. Transl. 7 (1971) 739.
[22] W. Schreyer, J.F. Shairer, Z. Kristallogr. Kristallgeom 116 (1961) 60.